Two-dimensional *XXZ*-Ising model on a square-hexagon lattice

J. S. Valverde, Onofre Rojas, and S. M. de Souza
Departamento de Ciências Exatas, Universidade Federal de Lavras, C.P. 3037, 37200-000 Lavras–Minas Gerais, Brazil
(Received 25 November 2008; published 1 April 2009)

We study a two-dimensional *XXZ*-Ising model on a square-hexagon (denoted for simplicity by 4–6) lattice with spin 1/2. The phase diagram at zero temperature is discussed, where five states are found, two types of ferrimagnetic states, two types of antiferromagnetic states, and one ferromagnetic state. To solve this model, we have mapped onto the eight-vertex model with union Jack interaction term, and it was verified that the model cannot be completely mapped onto eight-vertex model. However, by imposing an exact solution condition, we have found the region where the *XXZ*-Ising model on 4–6 lattice is exactly soluble with one free parameter, particularly for the case of symmetric eight-vertex model condition. In this manner we have explored the properties of the system and have analyzed the interacting competition parameters which preserve the region where there is an exact solution. Unfortunately the present model does not satisfy the *free fermion* condition of the eight-vertex model, unless for a trivial solution. Even so, we are able to discuss the critical point region, beyond the region of exact resolvability.

DOI: 10.1103/PhysRevE.79.041101 PACS number(s): 05.50.+q, 75.10.Jm, 05.30.−d, 05.10.−a

I. INTRODUCTION

Recently, frustrated magnetic systems have attracted a lot of attention due to their rich properties. Such systems have several phase diagrams displaying a number of unusual quantum phases [1,2]. Frustrated interactions are exhibited experimentally in inelastic neutron scattering. Therefore the two-dimensional magnetic lattice has become a challenge for theoretical investigation. After Onsager's [3] solution for the square two-dimensional Ising lattice, other solutions for regular two-dimensional lattices, such as triangular [4,5], honeycomb [6], kagome [7] lattice, and others, were explored in several works and their importance in statistical physics has encouraged physicists to search for a group of completely solvable models. The problem concerning the exact solution and the critical behavior of two-dimensional models were investigated by Fan and Wu [8,9]. In those works the *free fermion* (FF) condition and the free fermion approximation were studied in detail and the relations of Boltzmann weights for obtaining exact solvable models were established. In many situations where the FF condition is not satisfied completely it is possible to find restricted values of the parameters for which one can obtain a good approximation of the model. This is the case investigated by Tang [10], where the critical coupling of mixed Ising spin 1/2 with the arbitrary Ising spin S was studied using the free fermion approximation.

Since then, many theoretical investigations were developed, such as the Ising-Heisenberg kagome lattice [11,12], the quantum square-kagome antiferromagnetic lattice [13], the doubly decorated Ising-Heisenberg model [14], and the mixed-spin Ising model on a decorated square lattice with two different kinds of decorated spins on horizontal and vertical bonds [15]. Another exactly solvable Ising-model lattice known as square hexagon (4–6) was considered by Lin and Wang [16]. On the other hand different 4–6 lattices as a special case of the 4-8 lattices [17] were studied by Oitmaa and Keppert [18], where the solution for the Ising model with spin 1/2 was solved fully mapping into an eight-vertex model. It is remarkable that, the free fermion condition for the Boltzmann weights is satisfied identically in these models and the exact critical point can be obtained so that, the model falls within the standard Ising-model universality class.

Several real systems motivate the investigation of these kinds of lattices, such as the recently discovered two-dimensional magnetic materials $Cu_9X_2(cpa)_6\cdot xH_2O$ (cpa=2-carboxypentonic acid; X=F, Cl, or Br), where the Cu spins are situated on the triangular kagome lattice [19] with Heisenberg interaction type. Liquid crystal networks composed of pentagonal, square, and triangular cylinders [20]. Another recent investigation was about the crystal structure of solvated [Zn(tpt)2/3(SiF)(H20)2-(MeOH)] [tpt =2,4,6-tris(4-pyridyl)-1,3,5-triazine] networks with the (10,3)-a topology [21].

The present paper is organized as follows. In Sec. II we present explicitly the two-dimensional Hamiltonian of *XXZ*-Ising model on the 4–6 lattice. In Sec. III we study the phase diagram at zero temperature, showing some interesting phases. Section IV is devoted to the study of the exact solvable condition of the model, which is obtained by mapping onto symmetric eight-vertex model (SEVM) and the free fermion condition. Finally in Section V we give our conclusions.

II. TWO-DIMENSIONAL *XXZ*-ISING MODEL ON 4–6 LATTICE

In this paper we discuss the two-dimensional *XXZ*-Ising model on a square-hexagon (4–6) lattice, displayed schematically in Fig. 1. A single line represents the Ising interaction, whereas a double line represents the *XXZ* interaction. A similar lattice was discussed by Oitmaa and Keppert [18], where the interaction terms of the Hamiltonian were Ising interaction types [18] only.

The Hamiltonian of *XXZ*-Ising model on 4–6 lattice given in Fig. 1(a) can be expressed by

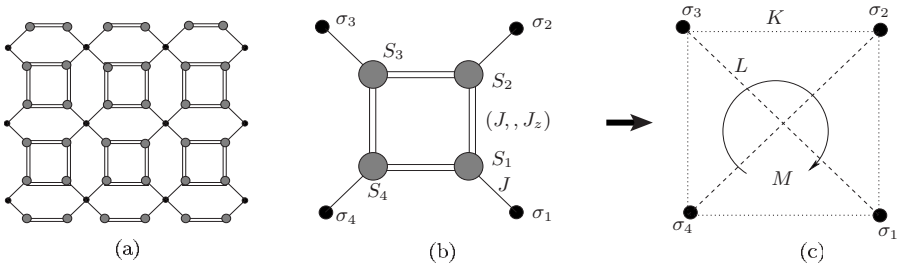

FIG. 1. Schematic representation of the two-dimensional *XXZ*-Ising model on 4–6 lattice. In (a) we represent by double line the *XXZ* interaction whereas with single line we represent the Ising interaction among particles with spin S_i and σ_i. In (b) we illustrate each decorated cell displayed in (a). In (c) we represent the transformation of unitary cell (b) into an effective square Ising model with nearest interaction parameter K, next-nearest interaction parameter L, and quartic interaction parameter M.

$$\mathcal{H}(\{\sigma\},\{S^{\alpha}\}) = \sum_{i} JS_i\sigma_i + \sum_{\langle i,j\rangle} [J(S_i^x S_j^x + S_i^y S_j^y) + J_z S_i^z S_j^z], \tag{1}$$

where the first summation runs over all sites involving the Pauli operator σ with two possible values ± 1, while the second summation with $\langle i,j\rangle$ runs over nearest neighbor of whole lattice containing the S^{α} spin-1/2 operators with $\alpha = \{x,y,z\}$.

III. PHASE DIAGRAM

The phase diagram at zero temperature for the two-dimensional *XXZ* Ising on 4–6 lattice is analyzed by computing the ground-state energy as a function of the model parameters. For each unitary cell [Fig. 1(b)], we diagonalize the square with the Heisenberg interaction coupling since the particles on each vertex of the square do not interact with squares of the other unitary cells. Fixing the values of spins $\{\sigma_1,\sigma_2,\sigma_3,\sigma_4\}$ in Fig. 1(b) we have 16 eigenvalues for each unitary cell. We use the rotation operator and spin inversion symmetry related to the spins $\{\sigma_1,\sigma_2,\sigma_3,\sigma_4\}$: (i) $\{+,+,+,+\}$, (ii) $\{+,+,+,-\}$, (iii) $\{+,+,-,-\}$, and (iv) $\{+,-,+,-\}$. These configurations are discussed in detail as follows.

A. Configuration {+,+,+,+}

Let us start by discussing the configuration $\{+,+,+,+\}$ of the energy levels. The square with Heisenberg coupling is the quantum Hamiltonian part of Eq. (1). To obtain the eigenvalues we need to diagonalize the second term of this Hamiltonian for each unitary cell, obtaining 16 eigenvalues. From that set of eigenvalues, we are able to find some energy levels that could become the ground-state energy for a given values of the parameters of Hamiltonian (1). Full eigenvalues of this configuration are given in the first column of Table I, while the second column gives the degeneracy of each eigenvalues.

One possible lowest eigenvalue is $\varepsilon_{\mathrm{FM}}=4J_z+4J$ for $J<0$ and its corresponding eigenstate is represented by

$$|\mathrm{FM}\rangle = \left|\begin{matrix} {}^{+}{}_{+}{}^{+} \\ {}_{+}{}^{+}{}_{+} \end{matrix}\right\rangle. \tag{2}$$

With large sign (+) (inner squared of signs) we represented the Heisenberg interaction particles with spin S, whereas by the corner small signals (+) we indicated the Ising interaction particles with spin σ. Since all spins are parallel, this state corresponds to the ferromagnetic state ($|\mathrm{FM}\rangle$).

Another possible lowest eigenvalue is given by $\varepsilon_{\mathrm{AF}_1}=4J_z-4J$ for $(J>0)$ and its corresponding eigenstate can be represented as

$$|\mathrm{AF}_1\rangle = \left|\begin{matrix} {}^{+}{}_{-}{}^{-}{}^{+} \\ {}_{+}{}^{-}{}_{-}{}^{+} \end{matrix}\right\rangle \tag{3}$$

using the same notation as above. The magnetization for the unitary cell is null; therefore this state corresponds to an antiferromagnetic state ($|\mathrm{AF}_1\rangle$).

Two further possible ground-state energies are $\varepsilon_{\mathrm{FI}^{\pm}}=\pm 6J$, for which in the square Heisenberg interaction the configuration becomes

$$|\mathrm{FI}^{\pm}\rangle = \sum_{r=0}^{3} (\pm \mathbf{R})^r \left|\begin{matrix} {}^{\pm}{}_{+}{}^{+}{}^{\pm} \\ {}_{\pm}{}^{-}{}_{+}{}_{\pm} \end{matrix}\right\rangle, \tag{4}$$

where $\mathbf{R}$ represents the rotation operator acting only on Heisenberg interaction particles with spin S. Each rotation is of $\frac{\pi}{2}$, around the axis perpendicular to the plane of lattice. The magnetization for the unitary cell is neither saturated; therefore, these states are known as ferrimagnetic. The ferrimagnetic state $|\mathrm{FI}^{+}\rangle$ has magnetization 3/4 and the ferrimagnetic state $|\mathrm{FI}^{-}\rangle$ has magnetization 1/4.

B. Configuration {+,−,+,−}

Another configuration which may eventually become the ground-state energy could be included in the configuration,

TABLE I. The energy levels of square Heisenberg coupling for the configuration $\{+,+,+,+\}$.

Energy $\{+,+,+,+\}$	Degeneracy
$\pm 6J$	1
$\pm 2J$	3
$4J_z \pm 4J$	1
$-4J_z$	1
0	3
$-2J_z \pm 2\sqrt{J_z^2+8J^2}$	1

TABLE II. The energy levels of the square Heisenberg coupling for the configuration $\{+,-,+,-\}$, with $j=0,1,2$.

Energy $\{+,-,+,-\}$	Degeneracy
0	3
$4J_z$	2
$\pm 2\sqrt{5}J$	2
$\pm 2J$	2
$-\frac{8}{3}[P_1\cos(\phi_j)-J_z]$	1

namely, $\{+,-,+,-\}$. To find the eigenvalues of this configuration, we need to diagonalize a matrix of dimension 16×16. This matrix can be obtained by fixing the magnetization $m_I=\sigma_1+\sigma_2+\sigma_3+\sigma_4$. The matrix then becomes blocked diagonal matrices, with the largest block matrix of 6×6. This block matrix can even be reduced due to rotation symmetry simply to a matrix of dimension 3×3, which reads

$$H_r=\begin{pmatrix} 4J-4J_z & 2J & 0 \\ 2J & 0 & 2J \\ 0 & 2J & -4J-4J_z \end{pmatrix}. \tag{5}$$

The eigenvalues of the reduced matrix H_r can be expressed as the roots of a polynomial of degree three, obtained from $\det(H_r-\varepsilon)$. The roots of the cubic equation read

$$\varepsilon_j=-\tfrac{8}{3}[P_1\cos(\phi_j)-J_z], \tag{6}$$

with $j=0,1,2$, whereas P_1 and ϕ_j are defined by

$$P_1=\sqrt{J_z^2+9J^2}, \tag{7}$$

$$\phi_j=\frac{1}{3}\cos^{-1}\left(\frac{J_z^3}{P_1^3}\right)+\frac{2\pi j}{3}. \tag{8}$$

The corresponding eigenstate is written as below,

$$|\mathrm{AF}_2\rangle=b_1\sum_{r=0}^{3}\mathbf{R}^r\left|{}^{+}_{-}{}^{++}_{--}{}^{-}_{+}\right\rangle+(1+b_2\mathbf{R})\left|{}^{+}_{-}{}^{+-}_{-+}{}^{-}_{+}\right\rangle, \tag{9}$$

and the coefficients of Eq. (9) are given explicitly by

$$b_1=\tfrac{1}{6J}[2P_1\cos(\phi_1)+J_z+3J], \tag{10}$$

$$b_2=\tfrac{4}{3J}b_1[P_1J\cos(\phi_1)-J_z]-1. \tag{11}$$

Here, there is only one antiferromagnetic state $|\mathrm{AF}_2\rangle$ which could be the ground state. We could say that this state is a frustrated state [22]. Particularly this lowest energy level is given by the eigenvalue $\varepsilon_1=-\frac{8}{3}[P_1\cos(\phi_1)-J_z]$.

All 16 energy levels presented in Table II can easily be obtained unless of those eigenvalues obtained from a reduced 3×3 matrix.

C. Configurations $\{+,+,-,-\}$ and $\{+,+,+,-\}$

The remaining configurations are $\{+,+,-,-\}$ and $\{+,+,+,-\}$. All these states have higher energy than the lowest energy states discussed above. In the first column of Table III, we explicitly give the eigenvalues of the configuration $\{+,+,-,-\}$ and the second column indicates the degeneracy of each eigenvalue. The energy levels for the configuration $\{+,+,+,-\}$ are given in the third column and in the fourth column the degeneracies of the energy are given.

TABLE III. The energy levels of the square Heisenberg coupling for the configurations $\{+,+,-,-\}$ and $\{+,+,+,-\}$, with $j=0,1,2$. The new parameters included in these eigenvalues are defined in Eqs. (12)–(15).

Energy $\{+,+,-,-\}$	Degeneracy	Energy $\{+,+,+,-\}$	Degeneracy
$4J_z$	2	0	2
$\pm 2J\pm\sqrt{2}J$	2	$\pm 2J$	1
0	1	$4J_z\pm 2J$	1
$-4J_z$	1	$-2J_z\pm B_+$	1
$\frac{J_z}{4}-P_2\pm A_+$	1	$-2J_z\pm B_-$	1
$\frac{J_z}{4}+P_2\pm A_-$	1	$\pm\frac{4J}{3}[4\cos(\theta_j)-1]$	1

The energy levels displayed in Table III use additional functions to express the energy level in a compact form. These functions are defined as follows:

$$\theta_j=\tfrac{1}{3}\cos^{-1}\left(\tfrac{5}{32}\right)+\tfrac{2\pi i}{3}, \tag{12}$$

$$P_2=\sqrt{J_z^2+10J^2+2J\sqrt{4J_z^2+25J^2}}, \tag{13}$$

$$A_\pm=\sqrt{\left(3\pm\frac{2J_z}{P_2}\right)(J_z^2+4J^2)+12J^2-P_2^2}, \tag{14}$$

$$B_\pm=2\sqrt{J_z^2+5J^2\pm 2J\sqrt{6J^2+J_z^2}}. \tag{15}$$

D. Zero temperature phase diagram

The ferromagnetic state ($|\mathrm{FM}\rangle$) given in Eq. (2) for $J_z<0$ is limited to $\frac{2}{5}J_z<J<0$. This state is depicted as orange region in Fig. 2. There is also an antiferromagnetic state ($|\mathrm{AF}_1\rangle$), represented by Eq. (3), for $J_z<0$, which is restricted to the interval $0<J<-\frac{2}{5}J_z$ and is displayed in Fig. 2 as a gray region. It is worth noticing that the state $|\mathrm{AF}_1\rangle$ behaves as a ferromagnetic for both Ising interaction particles with

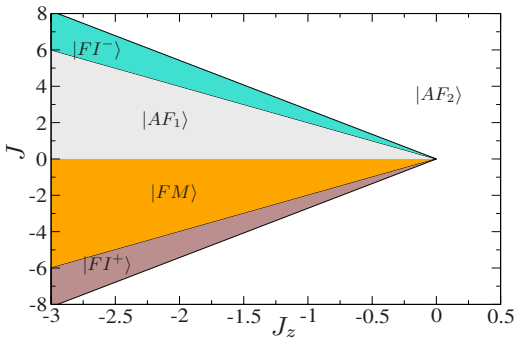

FIG. 2. (Color online) The phase diagram at zero temperature as a function of J_z and J.

spin σ and Heisenberg interaction particles with spin S, but with antiparallel orientation between them. Under the same conditions we also have two types of ferrimagnetic states (FI) which are explicitly given by Eq. (4): for $J_z<0$, the $|\mathrm{FI}^+\rangle$ is the ferrimagnetic state with magnetization 3/4, limited to $\frac{2}{5}J_z<J\leq 0.430\,675\,03J_z$, whereas the $|\mathrm{FI}^-\rangle$ corresponds to the ferrimagnetic state with magnetization 1/4, restricted by $-0.430\,675\,03J_z\leq J<-\frac{2}{5}J_z$. The value 0.430 675 03 is expressed numerically because in this situation we have a cumbersome transcendental equation, resulting from a root of a cubic equation [see Eq. (6)]. These regions are illustrated in Fig. 2 as brown ($|\mathrm{FI}^+\rangle$) and cyan ($|\mathrm{FI}^-\rangle$) regions. These ferrimagnetic states are invariant under whole exchange of spin orientation (σ and S).

The antiferromagnetic state $|\mathrm{AF}_2\rangle$ is present for arbitrary values of J when $J_z>0$, whereas for $J_z<0$ this state is limited by $|J|\geq -0.430\,675\,03J_z$, as illustrated in Fig. 2. We remark that in this case we have an antiferromagnetic interaction for both Ising and XXZ interaction particles.

We verify that there are five different states at zero temperature, as illustrated in Fig. 2. It is worth commenting that this model has a multicritical point at zero temperature, where the five states converge at $J=J_z=0$.

IV. MAPPING INTO AN EXACTLY SOLVABLE MODEL

To find a solution of Hamiltonian (1), one possibility is to map into a vertex model, which satisfies the exactly solvable condition of the eight-vertex model [23]. A similar mapping also was considered for studying the classical spin Ising model on 4–6 lattice; thus this model was solved exactly [18] by fully mapping into the eight-vertex model. However when quantum interaction term is included, solution becomes possible only for specific values of the parameters.

To study the thermodynamics of the model, we have written the partition function of the decorated XXZ-Ising model on 4–6 lattices, given by Hamiltonian (1) which reads as

$$\mathcal{Z}(\beta)=\sum_{\{\sigma\}=\pm 1}\mathrm{tr}_{\{S^\alpha\}}(e^{-\beta\mathcal{H}(\{\sigma\},\{S^\alpha\})}). \tag{16}$$

After taking the trace over operators $\{S^\alpha\}$ we have transformed the decorated XXZ-Ising model into an effective Ising model, with next-nearest and quartic interaction parameters, whose effective Hamiltonian may be expressed in general by

$$\tilde{\mathcal{H}}(\{\sigma\})=K\sum_{\langle i,j\rangle}\sigma_i\sigma_j+L\sum_{(i,j)}\sigma_i\sigma_j+M\sum_{\substack{\text{all}\\ \text{square}}}\sigma_1\sigma_2\sigma_3\sigma_4, \tag{17}$$

with K being the nearest-neighbor interaction, L being the next-nearest-neighbor interaction parameter, and M being the quartic interaction parameter. This transformation is also represented schematically in Fig. 1(c). The effective Ising model is the so-called "union Jack" lattice, which is an exactly solvable model [23].

Therefore the corresponding partition function of the effective Ising-model lattice is given by

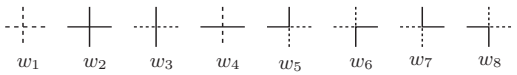

FIG. 3. The eight-vertex configurations [24]. Inversion of all spins corresponds to the same vertex.

$$\mathcal{Z}_{\mathrm{eff}}=f\sum_{\{\sigma\}=\pm 1}(e^{-\beta\tilde{\mathcal{H}}(\{\sigma\})}). \tag{18}$$

Using the Boltzmann weights displayed in Fig. 3, these are standard notations in the eight-vertex model [24]. Thus we are able to map Hamiltonian (1) into Eq. (17) where their parameters are related by the following expressions:

$$f=(w_1w_2w_3^2w_5^4)^{1/8}, \tag{19}$$

$$K=-\frac{1}{8\beta}\ln\left(\frac{w_1}{w_2}\right), \tag{20}$$

$$L=-\frac{1}{8\beta}\ln\left(\frac{w_1w_2}{w_3^2}\right), \tag{21}$$

$$M=-\frac{1}{8\beta}\ln\left(\frac{w_1w_2w_3^2}{w_5^4}\right). \tag{22}$$

Performing some algebraic manipulation we obtain cumbersome expressions for the associated Boltzmann weights of Hamiltonian (1). These large expressions are written using some additional functions which enable us to obtain a compact form. Those additional functions were already defined in Eqs. (7), (8), and (12)–(15),

$$w_1=3+e^{4\beta J_z}+8\cosh^3(2\beta J)+2e^{-4\beta J_z}\cosh(4\beta J)+2e^{-4\beta J_z}\cosh(2\beta\sqrt{J_z^2+8J^2}), \tag{23}$$

$$w_2=3+2e^{-4\beta J_z}+4\cosh(2\beta J)+4\cosh(2\sqrt{5}\beta J)+\sum_{j=0}^{2}\exp\left\{-\frac{8}{3}\beta[P_1\cos(\phi_j)-J_z]\right\}, \tag{24}$$

$$w_3=1+e^{4\beta J_z}+2e^{-4\beta J_z}+8\cosh(2\sqrt{2}\beta J)\cosh(2\beta J)+2\exp\left(\frac{\beta}{4}J_z\right)[e^{\beta P_2}\cosh(\beta A_+)+e^{-\beta P_2}\cosh(\beta A_-)], \tag{25}$$

$$w_5=2+2\sum_{j=0}^{2}\cosh\left[\frac{4\beta J}{3}(4\cos(\theta_j)-1)\right]+2e^{2\beta J_z}[\cosh(\beta B_+)+\cosh(\beta B_-)]+2\cosh(2\beta J)(1+e^{-4\beta J_z}). \tag{26}$$

The other Boltzmann weights can be obtained using the symmetry rotation. Our model satisfies the following identities for arbitrary parameter values:

$$w_3=w_4,\quad w_5=w_6=w_7=w_8. \tag{27}$$

In general the two-dimensional XXZ-Ising model on 4–6 lattices has no exact solution which fully maps onto the eight-vertex model, but it may be possible to find some re-

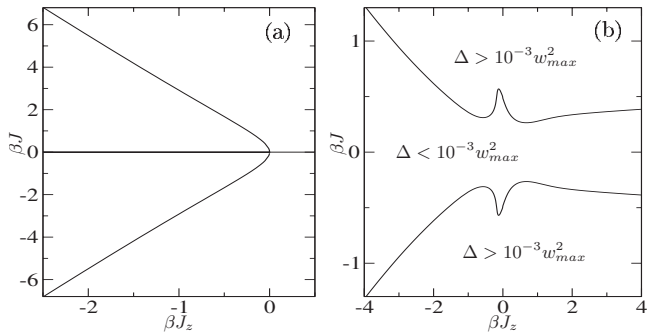

FIG. 4. In (a) the exactly solvable condition for SEVM ($w_1 = w_2$) is displayed. (b) The FF is imposed and there is no exact solution. However there is a wide valley where $\Delta/w^2_{\max} \ll 1$, particularly we show the region for $\Delta/w^2_{\max} > 10^{-3}$ as gray region.

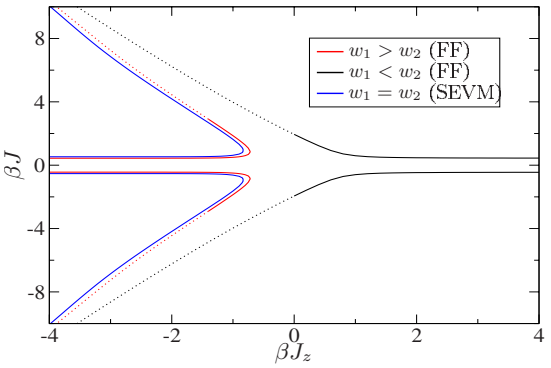

FIG. 5. (Color online) The critical point region under FF condition: red line corresponds to the condition of $w_1 > w_2$; black lines represent the condition when $w_1 < w_2$. Dotted line corresponds to the region where $\Delta/w^2_{\max} > 1$. When the SEVM condition is imposed, the critical region becomes curve given by the blue line.

stricted solutions imposing the exact solvable condition of the eight-vertex model. Therefore we will analyze the region where the model may have an exact solution.

A. Exactly solvable condition

An extensive study of the exactly solvable models is given in Ref. [24]. On the other hand, recently two-dimensional lattice models were solved mapping onto the eight-vertex model [11,12]. In general the mapping of our model into the eight-vertex model for arbitrary parameters of Hamiltonian (1) is not fully mapped onto the eight-vertex model. In what follows we will discuss these restricted mapping, where the model becomes solvable.

1. Symmetric eight-vertex model condition

The first branch of a possible exact solution could be obtained when the Boltzmann weights satisfy the so-called SEVM condition [23], where we must have the following relations:

$$w_1 = w_2, \quad w_3 = w_4, \quad w_5 = w_6, \quad w_7 = w_8. \tag{28}$$

Our model satisfies all the relations given by Eq. (28) except the first one [see Eq. (27)].

Imposing the first relation of Eq. (28) we have one possible solution with restricted parameters. In Fig. 4(a) we display the restricted parameter J as a function of the parameter J_z, where the exact solution under the SEVM condition is satisfied. Therefore we have shown that, for one free parameter, Hamiltonian (1) can be exactly solved; the transcendental equation involves a complicated relation among J_z and J. Therefore we are not able to invert one of the parameters explicitly as a function of the other one, but even so, we can invert numerically. In the limit of large values of J_z and J, we have the asymptotic limit where the relation is approximately given by $J = \pm 2.713\,579 J_z$. We also have a trivial solution when $J=0$; this corresponds just to a set of noninteracting square Ising models. For details see Hamiltonian (1).

2. Free fermion condition

The second candidate for an exact solution is the so-called FF condition [23] when the following relation,

$$\Delta = w_1 w_2 + w_3 w_4 - w_5 w_6 - w_7 w_8, \tag{29}$$

must satisfy the condition $\Delta = 0$.

Unfortunately on imposing the FF condition ($\Delta = 0$), we were unable to find a solution for the model given by Hamiltonian (1), except a trivial solution when $J=0$. In spite of Δ becoming a very cumbersome expression when $J \neq 0$, we are able to explore its behavior using algebraic software [25]. Thus we verified that in FF condition $\Delta/w^2_{\max}$ always has a positive amount. However, we can note that, when plotted for small $\Delta/w^2_{\max}$, the relation of J_z and J in units of β displays a wide valley which satisfies the condition $\Delta/w^2_{\max} \ll 1$, as depicted in Fig. 4(b), for $\Delta/w^2_{\max} < 10^{-3}$, whereas the gray region corresponds to the condition of $\Delta/w^2_{\max} > 10^{-3}$. This means that we can approximate our model to the FF condition and solve it with good approximation in the whole region of the valley.

B. Critical line

It is also possible to discuss the critical behavior even when an exactly solvable condition is not satisfied. For the first branch solution (SEVM), the critical condition must satisfy the following relation:

$$w_1 + w_3 + w_5 + w_7 = 2\ \max(w_1, w_3, w_5, w_7). \tag{30}$$

Thus in Fig. 5 we display the critical line region as a function of the parameters J and J_z in units of β, and we represent it by a blue solid line. The convergence for this case is satisfied in all critical points $|\Delta'|/w^2_{\max} < 1$, with $|\Delta'| = |w_1 - w_2|$ and $w_{\max} = \max\{w_1, w_2\}$.

The second branch of critical point region is obtained when we impose the FF condition,

$$w_1 + w_2 + w_3 + w_4 = 2\ \max(w_1, w_2, w_3, w_4). \tag{31}$$

In Fig. 5 we display the critical line region as a function of the parameters J and J_z in units of β, when the case of the Boltzmann weight w_1 is taken as the maximum value. The red solid line indicates the region where the FF approximation is valid ($|\Delta|/w_1^2 < 1$), and the red dotted line indicates the region where $|\Delta|/w_1^2 > 1$. The black solid line displays

the critical condition region when the w_2 is the largest one, with restriction $\Delta/w_2^2<1$, while the black dotted line represents the critical region when $\Delta/w_2^2>1$.

V. CONCLUSION

In this work we have discussed some particular solutions of two-dimensional *XXZ*-Ising model on a square-hexagon lattice. The decoration can be considered to be the square with an *XXZ* interaction and the interaction terms of the lattice are given by Ising-type coupling. We have discussed the phase diagram at zero temperature, displaying five different phases. To study the thermodynamics, imposing the exact solvable condition, the two parameters used originally were constrained. In this manner we have obtained a two-dimensional *XXZ* Ising on 4–6 lattice with one free parameter under the SEVM condition. Imposing the FF condition, we displayed a wide valley where the model could be considered to approximately satisfy the FF condition $\Delta/w_{\max}^2 \ll 1$. We have also discussed the critical condition even when the exact result condition was not satisfied. This model was fostered due to the recent discovery of real systems [19–21] with structures similar to those which we have considered in this work.

ACKNOWLEDGMENTS

J.S.V. thanks FAPEMIG for full financial support. O.R. and S.M.S. thank CNPq and FAPEMIG for partial financial support.

[1] J. Richter, O. Derzhko, and J. Schulenburg, Phys. Rev. Lett. **93**, 107206 (2004).
[2] J. Richter, J. Schuleburg, and A. Honecker, Lect. Notes Phys. **645**, 85 (2004).
[3] L. Onsager, Phys. Rev. **65**, 117 (1944).
[4] G. F. Newell, Phys. Rev. **79**, 876 (1950).
[5] K. Husimi and I. Syozi, Prog. Theor. Phys. **5**, 177 (1950).
[6] I. Syozi, Prog. Theor. Phys. **5**, 341 (1950).
[7] I. Syozi, Prog. Theor. Phys. **6**, 306 (1951).
[8] C. Fan and F. Y. Wu, Phys. Rev. B **2**, 723 (1970); Phys. Rev. **179**, 560 (1969).
[9] F. Y. Wu, Phys. Rev. **168**, 539 (1968); **183**, 604 (1969); Phys. Rev. B **4**, 2312 (1971).
[10] Kun-Fa Tang, J. Phys. A **21**, L1097 (1988).
[11] Dao-Xin Yao, Y. L. Loh, E. W. Carlson, and Michael Ma, Phys. Rev. B **78**, 024428 (2008).
[12] J. Strecka, L. Canova, M. Jascur, and M. Hagiwara, Phys. Rev. B **78**, 024427 (2008).
[13] Rahul Siddharthan and Antoine Georges, Phys. Rev. B **65**, 014417 (2001).
[14] Jozef Strecka and Michal Jascur, Phys. Rev. B **66**, 174415 (2002); Phys. Status Solidi B **233**, R12 (2002).
[15] J. Strecka, L. Canova, and M. Jascur, Phys. Rev. B **76**, 014413 (2007).
[16] K. Y. Lin and S. C. Wang, Phys. Lett. A **128**, 143 (1988).
[17] K. Y. Lin, Chin. J. Physiol. **26**, 150 (1988).
[18] J. Oitmaa and M. Keppert, J. Phys. A **35**, L219 (2002).
[19] R. E. Norman, N. J. Rose, and R. E. Stenkamp, J. Chem. Soc. Dalton Trans. **1987**, 2905; R. E. Norman and R. E. Stenkamp, Acta Crystallogr., Sect. C: Cryst. Struct. Commun. **46**, 6 (1990); M. Gonzalez, F. Cervantes-Lee, and L. W. ter Haar, Mol. Cryst. Liq. Cryst. Suppl. Ser. **233**, 317 (1993).
[20] B. Chen, Xiangbing Zeng, Ute Baumeister, Goran Ungar, and Carsten Tschierske, Science **307**, 96 (2005); G. Ungar and X. Zeng, Soft Matter **1**, 95 (2005).
[21] R. Robson, Dalton Trans. **2008**, 1039.
[22] J. S. Valverde, Onofre Rojas, and S. M. de Souza, J. Phys.: Condens. Matter **20**, 345208 (2008).
[23] R. J. Baxter and T. C. Choy, Proc. R. Soc. London, Ser. A **423**, 279 (1989).
[24] R. J. Baxter, *Exactly Solved Models in Statistical Mechanics* (Academic, New York, 1982).
[25] Any algebraic software, such as MAPLE, MATHEMATICA, or even a free software such as MAXIMA.